66-0768

JUNE 24, 1966

FIRST QUARTERLY PROGRESS REPORT

RESEARCH STUDY ON INSTRUMENT UNIT THERMAL CONDITIONING HEAT SINK CONCEPTS

MARCH 11 TO MAY 31, 1966

PREPARED FOR

GEORGE C. MARSHALL SPACE FLIGHT CENTER
HUNTSVILLE, ALABAMA
CONTRACT NO. NAS8-11291

GARRETT AIRESEARCH MANUFACTURING DIVISION
Los Angeles, California

66-0768

JUNE 24, 1966

FIRST QUARTERLY PROGRESS REPORT

RESEARCH STUDY ON INSTRUMENT UNIT THERMAL CONDITIONING HEAT SINK CONCEPTS

MARCH 11 TO MAY 31, 1966

PREPARED FOR

GEORGE C. MARSHALL SPACE FLIGHT CENTER
HUNTSVILLE, ALABAMA
CONTRACT NO. NAS8-11291

Prepared by: R. A. Stone
              D. W. Graumann

Approved by: ‾‾‾‾‾‾‾‾‾‾‾‾‾‾‾‾
             I. G. Austin

‾‾‾‾‾‾‾‾‾‾‾‾‾‾‾‾
F. E. Carroll

CONTENTS

FIGURES

FIRST QUARTERLY PROGRESS REPORT
RESEARCH STUDY ON INSTRUMENT UNIT
THERMAL CONDITIONING HEAT SINK CONCEPTS
MARCH II TO MAY 31, 1966

INTRODUCTION

This report reviews the work accomplished by the AiResearch Manufacturing
Division of The Garrett Corporation, Los Angeles, California, between March II
and May 31, 1966, under National Aeronautics and Space Administration
Contract NAS8-11291. This contract is for a research study on instrument unit
thermal conditioning heat sink concepts. This report is the first quarterly
progress report under the referenced contract which was signed on March II,
1966. The previous report under this contract was issued under AiResearch
report number 66-0612.

PROGRESS SUMMARY

In the first quarterly reporting period work was accomplished in the
following areas: Under Task I, Water Boiler Heat Sink Module, a review was
made of existing wick heat transfer endurance and wicking rate data from the
Apollo evaporator program and AiResearch Company sponsored work, and a litera-
ture review was made. A preliminary design of a wick module performance test
setup was completed, and detail drawings were started. Procurement of metal
felt wicks for testing was initiated. Under Task 2, Water Sublimator Heat
Sink Module, analysis of the mechanism and important design parameters of
sublimators was undertaken. Analysis of breakthrough pressure for both liquid
and vapor breakthrough was completed. A transparent sublimator was built and
tested in order to obtain a better understanding of the processes that occur
in sublimators. Design of a test apparatus for sublimation performance testing
of various porous plates was started, and a number of porous plates were pro-
cured for testing. Some bench tests were run on these plates.

PROBLEM DEFINITION

During the first two weeks of the program, effort was concentrated on
establishing a realistic problem definition, in order to ensure that the
parameters studied and module designs investigated will include the ranges of
interest to the NASA. The preliminary problem statement was reviewed at a

meeting at Marshall Space Flight Center on March 31, 1966. Participants in
the meeting were:

AiResearch	MSFC
P. J. Berenson	R. Huneidi
D. C. Collart	R. Wegrich
J. J. Killackey	J. Vaniman
L. B. Peltier	
R. A. Stone	

General concurrence in the problem statement defined in the following
paragraphs was obtained.

Hot Side Fluid

The hot side fluid will be representative of potential thermal
conditioning fluids. Within this broad range, the fluid for use in this
program will be selected on the basis of convenience and economy. Water and/or
ethylene glycol-water solution will be used in order to make maximum utili-
zation of existing test equipment.

Module Heat Load

The modules will be designed for maximum heat load of 3400 Btu per hr
(1 kw). The total maximum heat load for a typical application may be around
6 kw. The design, therefore, will permit module stacking to meet various
heat loads with the same design. Studies will include units that are capable
of meeting any heat load from 0 to full load, and also will include an inves-
tigation of the design simplifications that would be permitted with much less
variation in the heat load, say from full load to two-thirds load, for example.
All modules will be capable of a number of restarts.

Hot Fluid Inlet Temperature

The inlet temperature of the hot fluid will be varied between 45 and $90^\circ F$.
Outlet temperatures of $45^\circ F$ and $60^\circ F$ will be investigated, with control toler-
ances of $\pm 2^\circ$ and $\pm 5^\circ F$. While outlet temperatures in the range of $60^\circ F$ are of
greatest interest to the NASA, the outlet temperature will be treated para-
metrically. Transient changes in inlet temperature of up to 5 deg per min
will be investigated.

Operating Environment

The modules will be designed to operate in gravity environments from one g to zero g. Vibration environments typical of Saturn systems will be considered in the design. No vibration testing will be performed. This requirement will be accounted for by only using designs which are expected to be able to survive it. The ambient pressure for the modules will be hard-vacuum to 14.7 psia.

Required Operating Life

The units investigated will be capable of satisfying operational life-time requirements of from 4 hr to as much as 90 days. The effect of long duration operation on both sublimators and boilers will be considered.

Water Utilization Efficiency

The optimum water utilization can range anywhere from values around 40 percent to 100 percent depending on the length of mission, the cyclical operation of the evaporator, and the tradeoff between fixed weight and expendable weight. Water utilization will be treated parametrically; however, a goal of 90 percent minimum for long-duration systems will be considered.

Ground Test Attitude

Testing will include two attitudes with respect to gravity, namely, upward flow and downward flow. The results of this testing will be correlated with analytical predictions of the one g performance together with analysis of zero-g performance. This combination of analysis and testing is expected to lead to confidence that the modules will operate as required in gravitational fields ranging from zero g to one g.

DEVELOPMENT PLANS

Development plan outlines were prepared for Task 1, Water Boiler Heat Sink Module, and Task 2, Water Sublimator Heat Sink Module. These outlines are included as Tables 1 and 2, respectively. A development plan for Task 3, Thermal Conditioning Panel with Self-Contained Heat Sink, will be prepared later in the program at the conclusion of survey and analytical work on the water boiler and sublimator. Conceptual design of the thermal conditioning panels will probably derive from water boiler and sublimator design studies.

TABLE I

TASK I. WATER BOILER HEAT SINK MODULE DEVELOPMENT PLAN

Subtask

1. Establish Problem Statement and Test Plans

2. Wicking Investigation

    a. Review existing data

    b. Screen wicks of different kinds: nickel, CRES, fiberglass, etc. Investigate effects of density and thickness.

    c. Survey surface-active agents: EDTA, Sterox, etc. Determine effect of surfactant treatment upon wicking life, rate, height.

    d. Determine ability of various wicks to withstand wet-dry cycles.

    e. Determine susceptibility of various wicks to contamination. Identify contaminants by spectrographic and photographic means if possible. Devise means of reducing effect of contaminants.

    f. Determine reasonable engineering material specifications for wicks.

3. Water Flow Distribution

Analyze and test different water flow distribution techniques:

    a. Sponge-wick-porous plate

    b. Spray nozzles with flashing

    c. Effect of flow configuration (multipass, counterflow, etc.)

    d. Other

4. Water Flow Control

Analyze and test different means of controlling water flow within acceptable limits. Some possible control schemes are:

    a. Wick temperature sensor to control water in an on/off fashion

    b. Heat transport fluid outlet temperature sensor to control water in an on/off fashion.

TABLE I (Continued)

<u>Subtask</u>

    c.   Sense heat load (heat transport fluid inlet temperature) to fix
water on/off schedule.

    d.   Constant water flow

    e.   Other

5.   Heat Transfer Tests

Test single modules to determine heat transfer coefficient as a
function of pressure, wick material, wick thickness, and heat flux.
Use existing equipment to the extent possible.

6.   Temperature Control

Analyze and test different methods of controlling heat transport fluid
temperature. Some possible methods are:

    a.   Backpressure control to establish boiling temperature

    b.   Liquid bypass to limit heat transfer rate

    c.   Combinations, or other

7.   Module Geometry

Determine optimum module geometry and flow arrangement. Determine
method for selecting fins and wick-fin arrangement.

8.   Test Modules

Build and test modules based upon the above tasks, for heat transfer,
control, carryover, on-off, etc.

9.   Design Recommended Optimized Boiler Module

Heat Exchanger with controls, water supply, etc.

10.   Final Report

TABLE 2

TASK II WATER SUBLIMATOR HEAT SINK MODULE DEVELOPMENT PLAN

Subtask

1. Establish Problem Statement and Test Plan

2. Analysis

    a. Establish basic mechanisms

    b. Evaluate control schemes

    c. Develop porous plate specification

    d. Correlate results of bench tests with single module and three module sublimators

    e. Develop basic design techniques

    f. Optimize full-size sublimator design including control system

3. Procure Porous Plate Test Specimens

    a. Vendors to be considered:

        (1) Mott Metallurgical

        (2) Aircraft Porous Media

        (3) LMSC

        (4) Clevite

        (5) To be determined

    b. Possible materials:

        (1) Nickel

        (2) CRES

        (3) Monel

        (4) Nichrome

        (5) Noble metals and plastics

        (6) Titanium

TABLE 2 (Continued)

Subtask

    c.   Plate size shall be approximately 3.5 in. by 7.0 in. by 0.035 in. (to be used throughout test program)

    d.   Plates to be obtained with initial bubble point between 2.0 and 10.0 in. of mercury (with water). Water flow shall be maximum possible (greatest porosity).

4.   Porous Plate Bench Tests

    a.   Initial set of tests to include all or a portion of the following:

        (1)   Initial bubble point

        (2)   General bubble point (boiling pressure)

        (3)   Water flow at 1.0 in. Hg pressure differential

        (4)   Nitrogen pressure drop at 1.0 lb per min flow with discharge to ambient and 2.0 mm Hg abs

        (5)   Water retention pressure

        (6)   Flow uniformity

        (7)   Effect of surface treatment to produce nonwetting

5.   Single Module Testing

    a.   Basic goal will be to relate results of bench tests to actual sublimator performance. This data will then be used to optimize a full-size sublimator.

    b.   Test unit will incorporate one 3.5 in. by 7.0 in. porous plate and will use a constant heat flux electrical heater.

    c.   Tests will be run to determine the following:

        (1)   Maximum water supply pressure without liquid breakthrough

        (2)   Limits of mixed-mode operation

        (3)   Start-up characteristics

        (4)   Effects of surface treatments to promote hydrophobicity

TABLE 2 (Continued)

<u>Subtask</u>

        (5)   Effects of operation at minimum and zero heatload

        (6)   Effect of ambient pressure variation

        (7)   Transient response

        (8)   Effect of dissolved gases in water supply

  d.   Life tests will be run on selected single modules to evaluate effects of porous plate corrosion and/or microcontamination on sublimator performance. Porous plate selection will be guided by results of Apollo Air Trap Flow Degradation Testing. Tests will be run using single distilled water with one-half micron absolute filtration.

6.   Test Three-Module Sublimators

  a.   Design to be based on results of single module tests

  b.   Basic goal will be to develop a practical design using a fluid heat source with a predictable set of performance parameters. Tests will be run to evaluate the following:

        (1)   Start-up characteristics

        (2)   Overall performance

        (3)   Effect of water supply pressure on start-up and shut-down and steady-state performance

        (4)   Minimum heat load without complete freezing

        (5)   Maximum heat flux (maximum heat transport fluid inlet temperature)

        (6)   Transient response

        (7)   Operation with liquid bypass (Vernatherm) control

        (8)   Control concepts required to operate at zero heat load. Consider use of inlet temperature sensing to control water

TABLE 2 (Continued)

<u>Subtask</u>

flow. Allow unit to dry out at zero heat load by using residual heat capacity to sublime remaining water.

(9) Relationship to single module test results

7. Design Recommended Optimized Sublimator Module

Heat Exchanger with controls, water supply, etc.

8. Final Report

TASK I: WATER BOILER HEAT SINK MODULE

Review of Existing Wick Data

1.   Wick Endurance Testing

AiResearch has conducted a series of 1000-hr wick performance tests as
part of the Apollo glycol evaporator program. The series of tests of specific
interest involved 3 in. high by 6.4 in. wide nickel felt metal wicks of
15 percent density, with an average pore size of 0.00165 in. These wicks were
heated on both sides with electrical heaters separated from the wicks by off-
set rectangular fins. Four thermocouples were used to measure the plate
temperatures, two adjacent to the top half of the wick, and two adjacent to
the bottom half of the wick.

Five different types of tests were run. Two of the wicks were brazed as
received, two were oxidized at 800^0F in air and one was saturated with a 0.1
percent solution of Sterox NJ, a surface-active agent. To investigate the
effect of water filtration some of the samples were fed water that had gone
through a 10 micron filter, while the others were fed water that had gone
through one-half micron filtration. Table 3 shows the results. On the basis
of performance change, the best performance was obtained with the surfactant-
treated wick, which actually increased 19 percent in performance over the
1000-hr test. The best overall performance of the five specimens tested was
the brazed-as-received wick with one-half micron water filtration, which
declined in performance only 5 percent. The specimens which were fed 10
micron water had performance degradations of 51 percent and 36 percent,
respectively, while the oxidized wick which had one-half micron filtered
water, had a performance degradation of 23 percent. While the surfactant
apparently prevented any degradation and actually led to a significant increase
in performance with time, the effect of the surfactant was also to decrease
initial performance by a significant amount.

The following conclusions can be drawn from these 1000-hr tests.

a.   Water filtration and water purity is of great importance. Water
     that was filtered through a one-half micron filter led to much less
     degradation of wick performance than water which was filtered
     through a 10 micron filter.

TABLE 3. 1000 HR ENDURANCE TEST RESULTS 15% DENSE NICKEL FELTMETAL WICKS

| Wick Description	Location Number	$h_{initial}$ Btu/hr ft^2 °F	h_{final} Btu/hr ft^2 °F	$\dfrac{h_{final}}{h_{initial}}$	Average Performance Change
Brazed as received 10μ water filtration	Top 1	176	106	0.60	
	Top 2	240	66	0.28	
	Bottom 1	156	91	0.58	-51%
	Bottom 2	139	71	0.51	
Brazed as received 1/2μ water filtration	Top 1	203	240	1.18	
	Top 2	240	220	0.92	
	Bottom 1	120	106	0.88	-5%
	Bottom 2	132	106	0.80	
Brazed after heating in air, 800°F, 30 min 10μ water filtration	Top 1	83	61	0.75	
	Top 2	91	45	0.49	
	Bottom 1	102	66	0.65	-36%
	Bottom 2	102	66	0.65	
Brazed after heating in air, 800°F, 30 min 1/2μ water filtration	Top 1	106	80	0.76	
	Top 2	132	132	1.00	
	Bottom 1	91	64	0.71	-23%
	Bottom 2	115	71	0.62	
Brazed as received Saturated in 0.1 percent solution of Sterox NJ. 1/2μ water filtration	Top 1	61	126	2.04	
	Top 2	115	132	1.15	
	Bottom 1	115	78	0.68	+19%
	Bottom 2	115	102	0.88	

b. The oxidation of the nickel wicks in air leads to reduction in performance, and does not reduce susceptibility to degradation with time.

c. Treatment of wicks with surfactant may lead to considerable reduction in susceptibility of the wick to performance degradation with time. However, the surfactant may reduce the wicking rate of the wicks significantly. An interesting possibility would be to use wicks which had an initial wicking rate considerably in excess of that required, and treat these with surfactant. Based on the results of the above tests, it might be possible to obtain immunity from performance degradation, without the sacrifice of performance that would be obtained by treating the same wick with a surface active agent.

2. Wicking Rate

The following analysis develops an equation for time it takes liquid to reach various heights in a wick after the end of a dry wick has been brought into contact with the liquid. It is assumed that there is no heat or mass transfer from the sides of the wick; the flow rate of liquid is the same as each level at any one time.

Assuming that momentum changes are negligible reduces the force balance equation to three terms: gravity, friction, and surface tension. The pressure drop due to friction is equal to the pressure drop provided by the excess of capillarity over gravity:
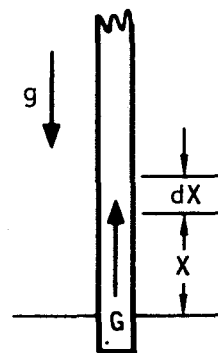
$$\frac{4\sigma \cos \theta}{D} - \frac{\rho g X}{g_0} = \frac{32\ C\ X\ \mu\ G}{\rho g_0 D^2} \tag{1}$$

The change of height with time is equal to the liquid velocity at any time. Combining this with the definition of mass velocity yields

$$G = \rho V = \rho\ \frac{dX}{dt} \tag{2}$$

Substituting Equation (2) into Equation (1) and solving for dt gives

$$dt = \frac{32\,\mu\,C}{g_0\,D^2}\;\frac{X\,dX}{\left(\dfrac{4\sigma\cos\theta}{D} - \dfrac{\rho g\,X}{g_0}\right)} \tag{3}$$

Integrating Equation (3) yields the final equation for the time it takes liquid to reach each height in the wick.

$$t_{g\neq0} = \frac{32\,\mu\,C}{\rho g\,D^2}\left[\frac{4\sigma\cos\theta\;g_0}{\rho g\,D}\,\ln\left(\frac{1}{1-\dfrac{\rho g\,D}{4\sigma\cos\theta\,g_0}}\right) - X\right] \tag{4}$$

Equation (4) shows that the time required to wick a height X is a function only of the pore diameter and fluid surface properties. Figures 1 and 2 show the results of wick rate tests at AiResearch. Table 4 lists the manufacturer's description of the wicks used in the tests of Figures 1 and 2.

TABLE 4

FELTMETAL WICK PORE SIZE

Material	Density	Average Pore Size, in.	Maximum Pore Size, in.	Pore Size Range, in.
Stainless Steel	15%	.00140	.00200	.00100 – .00180
Nickel	15%	.00165	.00264	.00075 – .00189

The manufacturer of the wicks, Huyck Metals, claims that less than 1 percent of the pores are larger than the indicated maximum pore size and that 80 percent of the total pore volume is within the indicated pore size range. Figure 1 shows wick rate tests for 15 percent dense, stainless steel Feltmetal. On Figure 1 are shown wick rate tests for four different wick thicknesses ranging from 0.015 in. to 0.125 inch. The data shows a marked influence of wick thickness on wicking rate. Also plotted on Figure 1 are the wick rates predicted by Equation (4) for a value of cos θ equal to 0.5, and C, the tortuosity of the pores, equal to 1.5. These numbers represent little more than guesses, but they should be conservative. The three lines for Equation (4) represent wicking time versus height for the nominal minimum pore size, the average pore size, and the maximum pore size. It is seen that the wick rates predicted for the nominal maximum pore size fall fairly close to the wick rate with the thickest wick. A possible explanation
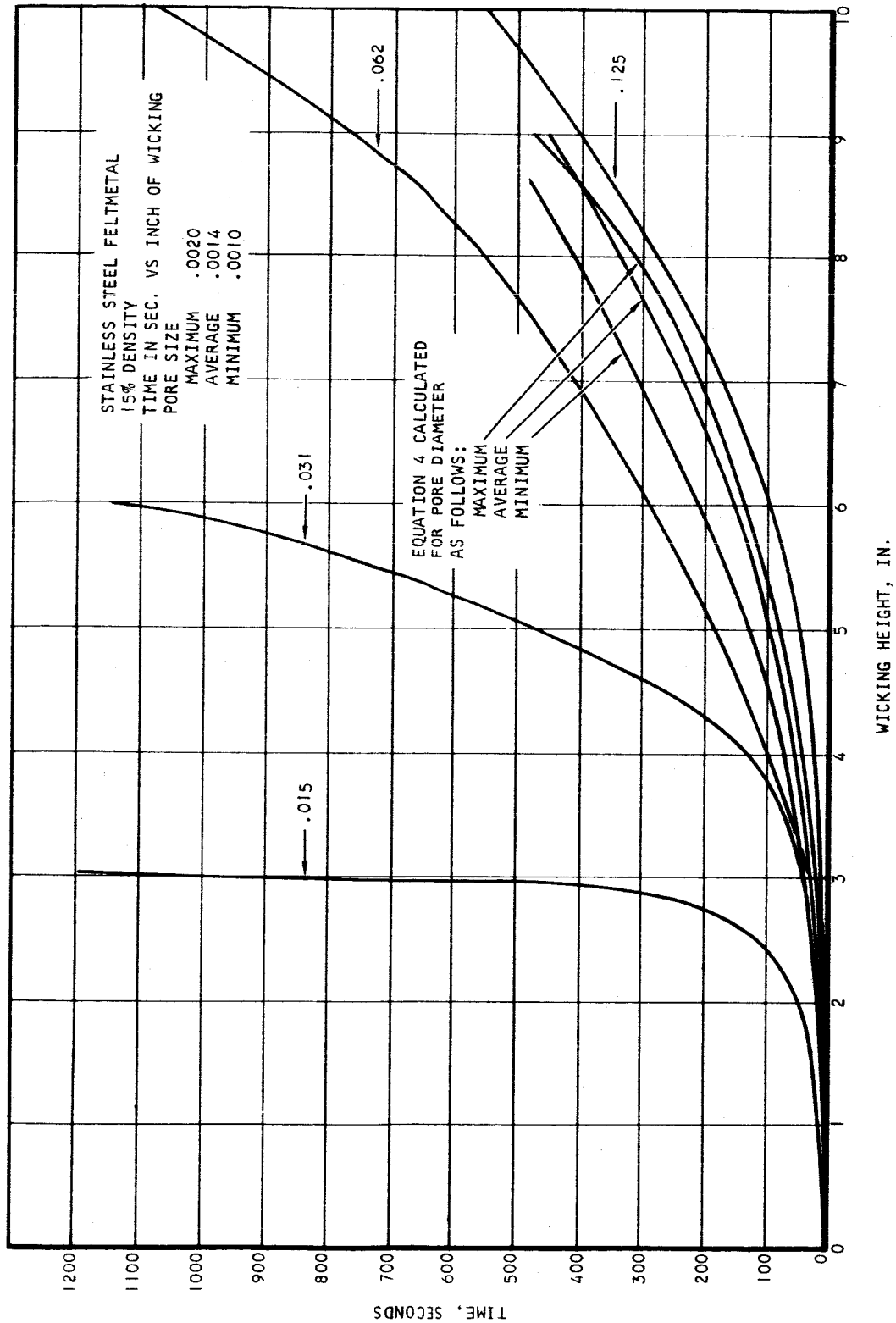
Figure 1. Wicking Height vs Elapsed Time for Stainless Steel Wicks

The chart axes and annotations:

- X-axis: WICKING HEIGHT, IN.
- Y-axis: TIME, SECONDS

STAINLESS STEEL FELTMETAL
15% DENSITY
TIME IN SEC. VS INCH OF WICKING
PORE SIZE
  MAXIMUM   .0020
  AVERAGE   .0014
  MINIMUM   .0010

EQUATION 4 CALCULATED
FOR PORE DIAMETER
AS FOLLOWS:
  MAXIMUM
  AVERAGE
  MINIMUM
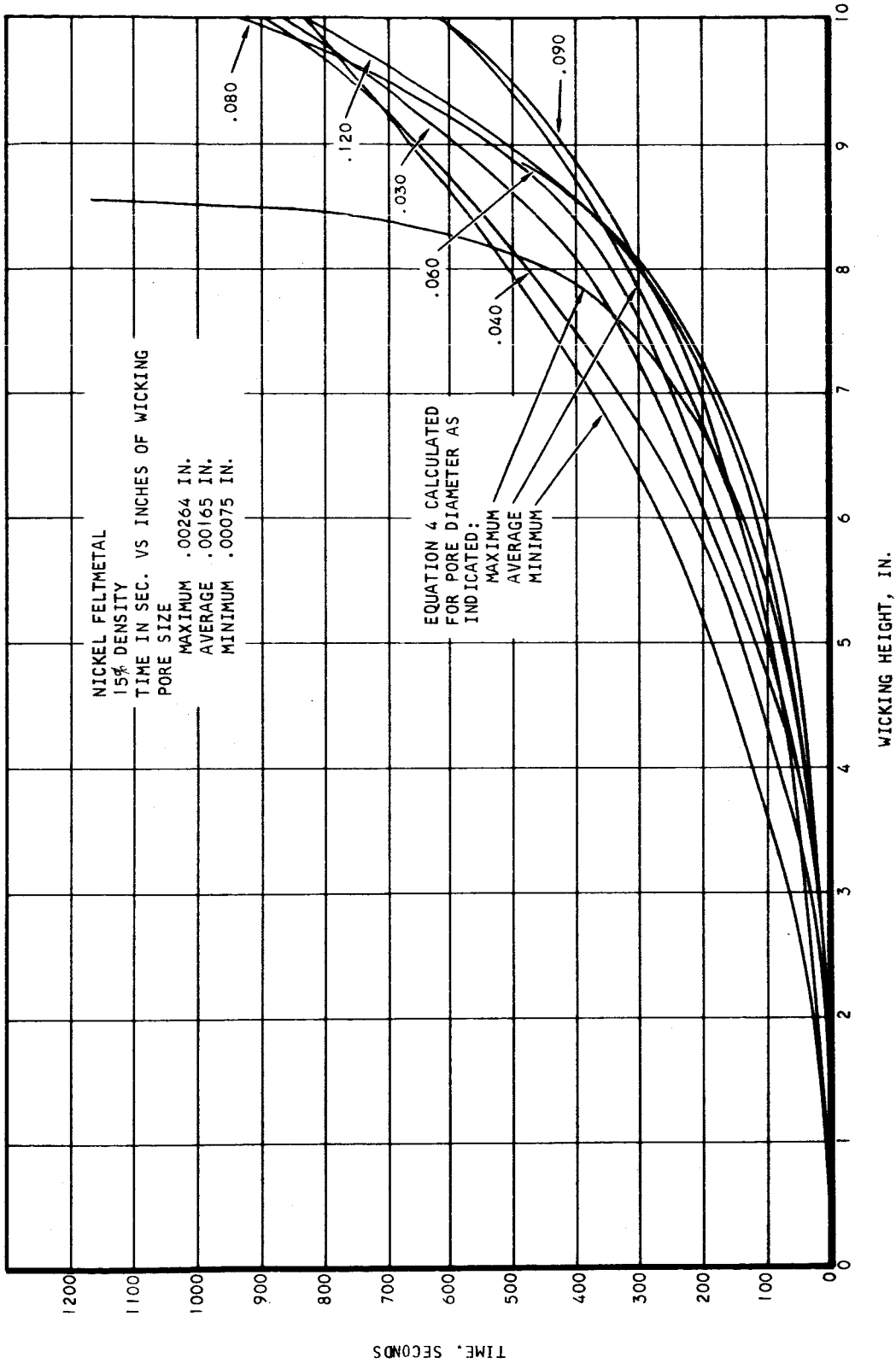
B-11030

Figure 2. Wicking Height vs Elapsed Time for Nickel Wicks

B-11031

for the effect of wick thickness on wick rate may be the surface treatment of the wick. That is, the way the wick is rolled or pressed may close or reduce in size some of the pores near the surface. If this were the reason it would mean that thicker wicks are less influenced by thickness than thin ones, which is seen from both Figures 1 and 2 to be the case in the AiResearch experiments. Another reason for the thin wicks having a greatly reduced wicking capability may be contamination, probably from the atmosphere. This might also be a surface effect; that is the contaminants penetrate deeper fractionally into the thin wicks than the thick ones. Figure 2 shows the same results for 15 percent dense nickel Feltmetal. Here the spread between the various wick thicknesses is still pronounced, though not nearly as wide as was the case for stainless steel. This could indicate that nickel is less easily contaminated than stainless steel. The analytical curve for the nominal pore size of 0.00165 in. in Figure 2, falls very close to the measured wick rate for the 0.090 in. wick, which is the one most commonly used in evaporators at AiResearch.

The tests reported above were run before it was fully appreciated how easily susceptible the wicks are to contamination and how extreme the requirement for cleanliness was. Later in this program wick rate tests will be repeated under a more carefully controlled environment. The capacity of the wicks to deliver water in an evaporator is one of the most important design parameters, and it is essential that the wick rate capacity be understood and predictable.

Wick Heat Transfer and Performance Testing

A preliminary design of a wick module performance test setup was prepared, and detail drawings are about 50 percent completed. This design will allow for testing of wicks of different thicknesses and wick height, using steam fins of varying geometry, in particular, rectangular and triangular fins. Wicks of different porosity will be tested, and the test section will be capable of varying electrical heat input to vary heat flux. Electrical heating was selected over fluid heating for simplicity of operation, and better heat balances. The electrical heaters will be attached to a heavy copper plate so as to permit fairly exact definition of the temperature boundary conditions. The heater will be made in several vertical sections, so that the rate of heat input can be varied along the wick as would be the real situation in a wick water boiler that was removing heat from a fluid stream.

Procurement of wicks to be tested has been initiated. Nickel, stainless steel, monel, copper and possibly aluminum wicks will be obtained. The material will cover a wide range of thicknesses and densities.

TASK II: WATER SUBLIMATOR HEAT SINK MODULE

Sublimator Analysis

According to the theory presented in Reference 1, the sublimation mechanism is characterized by a layer of ice on the inside face of the porous plate. The existance of this ice layer is determined by a combination of the vapor pressure drop characteristics of the porous plate and the heat flux or vapor flow rate. When the vapor pressure drop across the porous plate is less than the triple point pressure the phase change must be from the solid directly to the vapor phase, by sublimation of the ice layer. The thickness of the ice is governed by the rate of heat transfer and the sublimation temperature corresponding to the local vapor pressure at the inlet face of the porous plate. To meet the imposed heat load the ice sublimes at the face of the porous plate and freezes at a corresponding rate at the liquid interface. The generated vapor passes through the porous plate. It can be shown that the normal operating pressure differentials across the porous plate and ice layer are insufficient to extrude the ice into the pores and thus the ice forms a barrier to liquid flow into the pores.

If the input heat flux is increased, the vapor pressure drop across the porous plate increases causing the sublimation temperature to rise accordingly. This results in a reduction in the ice layer thickness in order to satisfy the heat conduction requirements. Eventually the ice layer will disappear completely when the heat flux is sufficient to cause the vapor pressure at the inlet face of the porous plate to be greater than the triple point pressure. It is at this point that the evaporation mechanism begins to occur. However, if the pore size distribution is non-uniform, the heat flux at which this transition occurs will vary with location on the plate due to inequalities in vapor pressure drop, resulting in mixed mode operation.

Typical porous plates contain a random distribution of pores with respect to both size and shape. The point of transition for any single pore is dependent on its equivalent radius and ultimately the vapor pressure drop produced

[1]Porous Plate Water Boiler Design Study - Final Report, HSER 3509, Hamilton Standard Division of United Aircraft Corporation, Windsor Locks, Connecticut, May 20, 1965.

by the pore. In the mixed mode of cooling, phase change occurs at local temperatures above and below the triple point depending on the local pore geometry. An averaging effect exists and if the plate is of reasonable thermal conductivity the effective plate temperature remains constant and very near $32^\circ F$ over a wide range of heat flux. Design calculations are then simply based on a triple point sink temperature.

The main elements of the theory are summarized above. Some portions of this theory, however, are not consistent with the experimental data given in Reference 1 or the observations made here at AiResearch. In order to formulate a more consistent theory several "mixed mode" models were proposed and analyzed to check their validity.

The original model assumed both sublimation and boiling taking place at the upstream face of the porous plate with all the vapor passing through the entire plate. Using this model, a pressure drop corresponding to the vapor flow rate fixed by the experimental heat flux may be determined from pressure drop vs flowrate data. This was done for several test modules referred to in Reference 1.

From the experimental heat flux, the vapor mass flux is determined from the equation:

$$W = \frac{Q/A}{\Delta H_s} \tag{5}$$

where W = vapor mass flux, lb_m/hr ft^2

Q/A = Heat flux, Btu/hr ft^2

ΔH_s = Heat of sublimation of water, Btu/lb_m

By using experimental nitrogen flow rate vs pressure drop curves for free molecule flow given in the referenced report, and by making a simple water vapor correction (given below) derived from the free molecule pressure drop equation, the pressure drop through the porous plate may be determined.

$$\Delta P_{vapor} = \Delta P_{N_2} \left(\frac{R_{vapor}}{R_{N_2}} \right)^{1/2} = 1.25\ \Delta P_{N_2} \tag{6}$$

ΔP_{vapor} = Water vapor pressure drop, lb_{f/in^2}

ΔP_{N_2} = Nitrogen pressure drop, lb_{f/in^2}

R_{vapor} = Water vapor gas constant = 85.8 lb_f ft/lb_m °R

R_{N_2} = Nitrogen gas constant = 55.2 lb_f ft/lb_m °R

The experimental data and calculated pressure drops are given in Table 5. It is seen that the pressure drops obtained in this manner give pressures on the upstream side of the porous plate of from 1.5 to 11 times the triple point pressure. Since ice was observed in the test units, these high pressures obviously could not have been attained, indicating a deficiency in the assumed mechanism.

In order to account for this pressure drop discrepancy, the model was revised, proposing sublimation at the upstream face and boiling near the downstream face. This is essentially the theory given in Reference 1 for "mixed mode" operation. According to this reference, sublimation takes place upstream because the pressure differential is not sufficient to extrude the ice layer into the pores, and the vapor generated passes through the entire plate. Boiling takes place inside the plate, at or near the downstream face giving a small pressure drop. In effect, this model suggests sublimation over some areas of the plate with pressure drop and boiling over the remaining areas with negligible pressure drop, the difference arising from the different sides of the plate at which phase change occurs.

The validity of this model may be tested by experimentally determining the average heat flux over the plate, from this determining the relative magnitudes of the boiling and subliming heat fluxes, and observing whether the values obtained are reasonable. This was done for several test plates from the reference as shown below. The total average heat rate is equal to the sum of the boiling heat rate and the subliming heat rate.

TABLE 5

CALCULATED PRESSURE DROP FOR VAPOR FLOW THROUGH
POROUS PLATES IN SUBLIMATOR

Porous Plate	Q/A Btu/hr ft^2	P$_{ambient}$ psi	T$_{pp}$ °F	W lb/hr ft^2	ΔP_{vapor} psi
C	470	0.001	33.7	0.385	0.36
	710		34.0	0.582	0.51
	970		34.2	0.795	0.69
	1230		32.0	1.01	0.87
	1475		31.8	1.21	1.03
D	420	~0.002	30.5	0.344	0.131
	475		28.9	0.389	0.140
	580		31.5	0.475	0.156
	610		33.7	0.500	0.162
	690		31.2	0.565	0.168

Q/A = experimental heat flux

P$_{ambient}$ = pressure in vapor passage

T$_{pp}$ = porous plate temperature

W = calculated vapor mass flux

ΔP_{vapor} = calculated vapor pressure drop based upon assumption that vaporization takes place at water side porous plate face

$$q_s A_s + q_B A_B = q_{avg} A_T \tag{7}$$

where q_s = subliming heat flux

q_B = boiling heat flux

q_{avg} = average heat flux, experimentally determined value

A_s = area over which sublimation takes place

A_B = area over which boiling takes place

A_T = total plate area = $A_s + A_B$

By defining a "boiling area ratio" $(R_B = \dfrac{A_B}{A_T})$ which is the ratio of the plate area over which boiling takes place to the total plate area and dividing both sides of (7) by A_T, one obtains

$$q_s (1 - R_B) + q_B R_B = q_{avg} \tag{8}$$

which becomes:

$$\frac{q_B}{q_s} = \frac{1}{R_B} \left[R_B - 1 + \frac{q_{avg}}{q_s} \right] \tag{9}$$

For a given plate with a known pressure drop as a function of vapor flux, one may determine the maximum possible flow rate per unit area, w_s, which gives a pressure drop low enough to keep the upstream pressure at or below the triple point pressure, thereby assuring the possibility of ice (and sublimation) at the upstream face. This flow rate is then the maximum possible vapor flux over the subliming area, and from this, the sublimation heat flux may be found.

$$q_s = \Delta H_s w_s \tag{10}$$

ΔH_s = heat of sublimation

w_s = vapor flow rate per unit area

Once q_s is known, Equation (9) may be solved for $\dfrac{q_B}{q_s}$ using values of R_B between

0 and 1. The ratio of boiling heat flux to subliming heat flux was calculated for the referenced published experimental data and typical results are given below for plate D with an experimental average heat flux of 420 Btu/hr ft².

$q_s \frac{Btu}{hr\ ft^2}$	Assumed R_B	q_B/q_s
120	1.0 (maximum possible)	3.44
120	0.9	3.72
120	0.8	4.05
120	0.7	4.49

This analysis indicates that the heat flux over those areas at which boiling takes place is 3 to 5 times greater than the heat flux existing over the subliming areas. In order to support such great variation in heat flux, there must be either a correspondingly great variation in the local heat transfer resistance between the heated surface and porous plate or a large variation in the local source temperature. Since neither of these seems likely in the test modules used, and neither was reported along with the experimental data, it can only be assumed that the model of sublimation and boiling occurring upstream and downstream of the porous plate, respectively, is inaccurate.

The model currently under consideration is that of sublimation taking place not at the upstream face but within the pores cyclically, with the ice vapor interface receding and again forming when water fills the pores and freezes. Sublimation visualization tests which will be explained below seem to lend credibility to this model.

The importance of where the phase change occurs and, therefore, the magnitude of the vapor pressure drop becomes increasingly obvious when a design is considered. If a conservative design is made, assuming vaporization at the upstream plate face and allowing sufficient plate area to limit the upstream pressure to a value below the triple point, the porous plate area, using conventional plates, is by far the controlling factor in the design, causing the unit to be from 5 to 20 times larger than the heat transfer requirements would dictate.

Capillary Flow and Breakthrough Analysis

An analysis of flow in capillaries was undertaken. Rate of liquid rise and final rise height in capillary tubes are reasonably well understood.

However, phenomena occurring at the boundary of both wicks and porous plates are not well enough understood to permit optimum design of hardware. Two questions of considerable importance that have not been defined as yet are (1) why does a wick filled to less than its maximum wick height drip when it is removed from a water surface and under exactly what conditions? and (2) how can bubble point and liquid breakthrough of porous plates be related to pore geometry, surface tension, and contact angle? Measurements of liquid breakthrough of porous plates in the literature have shown that the breakthrough pressure can vary from a very small fraction of the gas breakthrough pressure to a number in excess of the gas breakthrough pressure. To better understand this situation an analysis of the phenomena of breakthrough of both liquid and gas was undertaken and some preliminary results for a specific pore geometry and range of contact angles were presented in the last monthly report. Additional analysis has been performed and revisions made.

This further analysis involves the phenomena of liquid and vapor breakthrough for capillary tubes with rounded exits of various sharpnesses and for contact angles from 0 to 180 degrees. The reason for investigating various exit sharpnesses is that in a porous plate of conventional construction, a sharp cornered capillary will not be the typical pore geometry. A sketch of the axially symmetrical model used in the analysis is shown below.
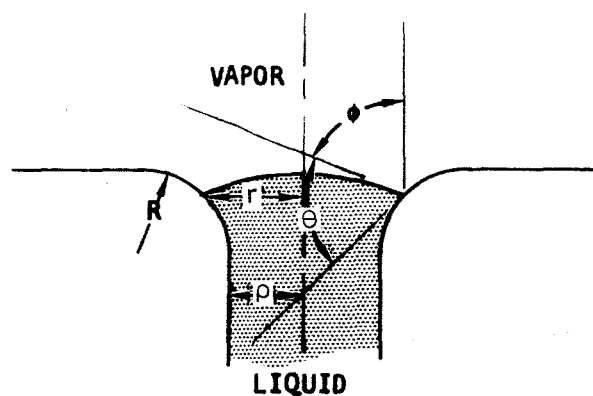
A-21705

Admittedly, the pore exits in a porous plate will probably not have symmetrical shapes; nevertheless, it is felt that the following analysis is useful in that it provides a better understanding of the breakthrough phenomenon and gives an idea as to the desirable plate and fluid-surface characteristics. For clarity,

the following analysis is given for liquid breakthrough; however, it can be shown that the results for liquid breakthrough with a contact angle of θ are the same as those for vapor breakthrough for an angle of $180° - \theta$.

A force balance on the vapor-liquid interface gives for $\rho \leq r \leq \rho + R$:

$$P_L - P_V = \frac{2\sigma}{r} \cos \phi \qquad (11)$$

where P_V = the pressure on the vapor side

P_L = the pressure on the liquid side

σ = the surface tension

From simple geometric relations, one obtains $\cos \phi$ as a function of contact angle θ, r, ρ, and R; therefore, the expression for the interface pressure differential becomes:

$$P_L - P_V = \frac{2\sigma}{r} \left\{ - [1 - (\frac{\rho}{R}) (\frac{r}{\rho} - 1)] \cos \theta + [2 (\frac{\rho}{R}) (\frac{r}{\rho} - 1) - (\frac{\rho}{R})^2 (\frac{r}{\rho} - 1)^2]^{1/2} \sin \theta \right\} \qquad (12)$$

If both sides of (12) are divided by $\frac{2\sigma}{\rho}$, one obtains the normalized pressure differential $\frac{P_L - P_V}{\frac{2\sigma}{\rho}}$. For vapor breakthrough the equation for the interface pressure differential is the same as (12) except there is no minus sign on the coefficient of the $\cos \theta$ term. Therefore since $\cos (180 - \theta)$ is equal to $- \cos \theta$, the vapor breakthrough pressure for $180 - \theta$ is equal to the liquid breakthrough pressure for a contact angle of θ.

For a given contact angle θ and "exit sharpness" $\frac{\rho}{R}$, the ratio of the pore radius to the radius of curvature of the exit, one can evaluate the normalized pressure differential $\frac{P_L - P_V}{\frac{2\sigma}{\rho}}$ for different values of r between ρ and $\rho + R$ from Equation (12), and upon doing so, observes that the normalized pressure differential increases and then decreases with increasing r. An example of this is shown in Table 6 for an "exit sharpness" of 1.0 and a contact angle of 100 degrees.

TABLE 6

NORMALIZED PRESSURE DIFFERENTIAL ACROSS LIQUID-VAPOR INTERFACE
FOR EXIT SHARPNESS OF 1.0 AND CONTACT ANGLE OF 100 DEG

r/ρ	$\cos \phi$	$\dfrac{P_L - P_V}{\dfrac{2\sigma}{\rho}}$
1.00	0.174	0.174
1.05	0.474	0.451
1.10	0.860	0.532
1.20	0.700	0.584
1.30	0.825	0.634
1.40	0.892	0.637 ← Breakthrough occurs at this value of r/ρ
1.50	0.940	0.626
1.60	0.972	0.607
1.70	0.991	0.583

One notes that for this case the maximum value of $\dfrac{P_L - P_V}{\dfrac{2\sigma}{\rho}}$ occurs at $r = 1.4\ \rho$.

The maximum normalized pressure differential will occur at different values of r/ρ for different combinations of θ and $\frac{\rho}{R}$. The maximum value of $\Delta P / \frac{2\sigma}{\rho}$ is the normalized breakthrough pressure, for if this ΔP is exceeded, the liquid will detach from the capillary opening and breakthrough will occur. To obtain the breakthrough pressure P_B for a given θ and $\frac{\rho}{R}$, one first solves for the $\frac{r}{\rho}$ at which breakthrough occurs. This is done by differentiating Equation (12) with respect to $\frac{r}{\rho}$.

$$\frac{d\left(\dfrac{P_L - P_V}{2\sigma/\rho}\right)}{d\left(\dfrac{r}{\rho}\right)} = -\left(\frac{\rho}{r}\right)^2 \left(1 + \frac{\rho}{R}\right)\cos\theta + \left(\frac{\rho}{r}\right)\left[2\frac{\rho}{R}\left(\frac{r}{\rho} - 1\right) - \left(\frac{\rho}{R}\right)^2\left(\frac{r}{\rho} - 1\right)^2\right]^{1/2}$$

$$\left[\frac{\dfrac{\rho}{R}\left(1 - \dfrac{r}{R} - \dfrac{\rho}{R}\right)}{2\dfrac{\rho}{R}\left(\dfrac{r}{\rho} - 1\right) - \left(\dfrac{\rho}{R}\right)^2\left(\dfrac{r}{\rho} - 1\right)^2} - \frac{\rho}{r}\right]\sin\theta$$

(13)

Equation (13) is then set equal to zero and solved for $\frac{r}{\rho}$. This value is then substituted into (12) and the normalized breakthrough pressure $\frac{P_B}{2\sigma/\rho}$ is found.

The results of this analysis are shown in Figure 3 for "exit sharpnesses" of 0, 0.1, 0.5, 1.0, 3, and ∞. As previously stated, results for vapor breakthrough correspond to liquid breakthrough for the supplementary contact angle. One notes that for an infinitely sharp corner, the liquid breakthrough pressure is independent of θ between 90 and 180 deg and proportional to $\sin \theta$ between 0 and 90 deg. For a sharpness ratio of 0, the curve takes the form of a cosine curve. Liquid breakthrough pressure is seen to decrease with decreasing contact angle and exit sharpness ratio. Another interesting feature of this plot is that for values of θ to the right of the diagonal broken line, the normalized breakthrough pressure may be represented exactly by by $\frac{P_B}{\frac{2\sigma}{\rho}} = \frac{\sin \theta}{1 + \frac{R}{\rho}}$. The reason for this simplified expression has to do with the point in the capillary exit at which the breakthrough pressure is reached, and this will be explained below.

Figure 4 shows the position of the interface prior to liquid breakthrough for a pore with a sharpness ratio of 0.5 for various contact angles. One notes that as the contact angle is decreased, the point of contact moves further out of the pore until it reaches the outer extremity where $\frac{r}{\rho} = 1 + \frac{R}{\rho}$. Upon further reduction of the contact angle, the vapor liquid interface contacts the pore wall at the same location. The maximum contact angle for breakthrough at $\frac{r}{\rho} = 1 + \frac{R}{\rho}$ is given by:
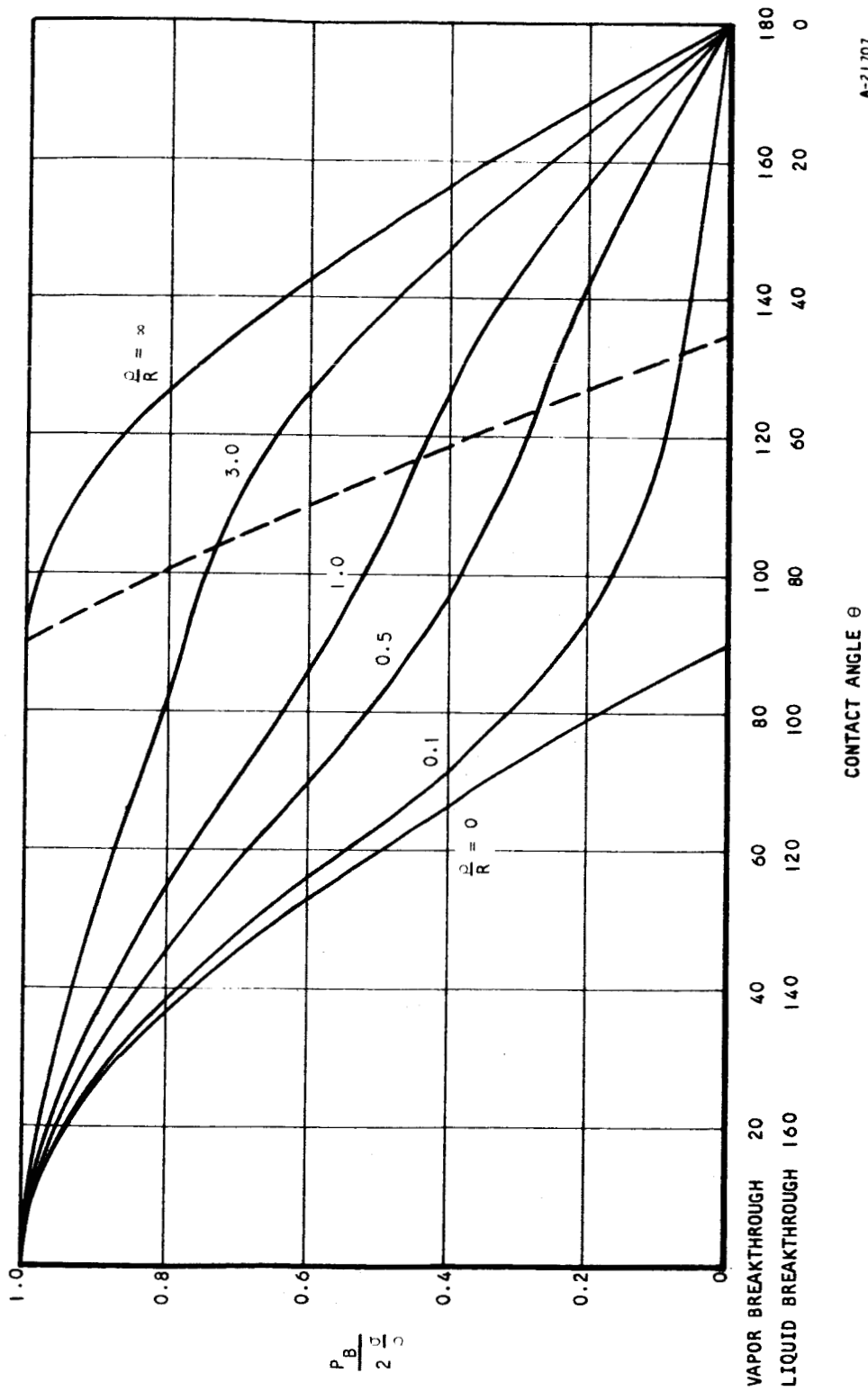
$$\theta_{max} = \arctan \left(1 + \frac{\rho}{R} \right) \tag{14}$$

This means that for all angles less than θ_{max}, breakthrough will occur at $\frac{r}{\rho} = 1 + \frac{R}{\rho}$ and the defining equation obtained from a force balance is:

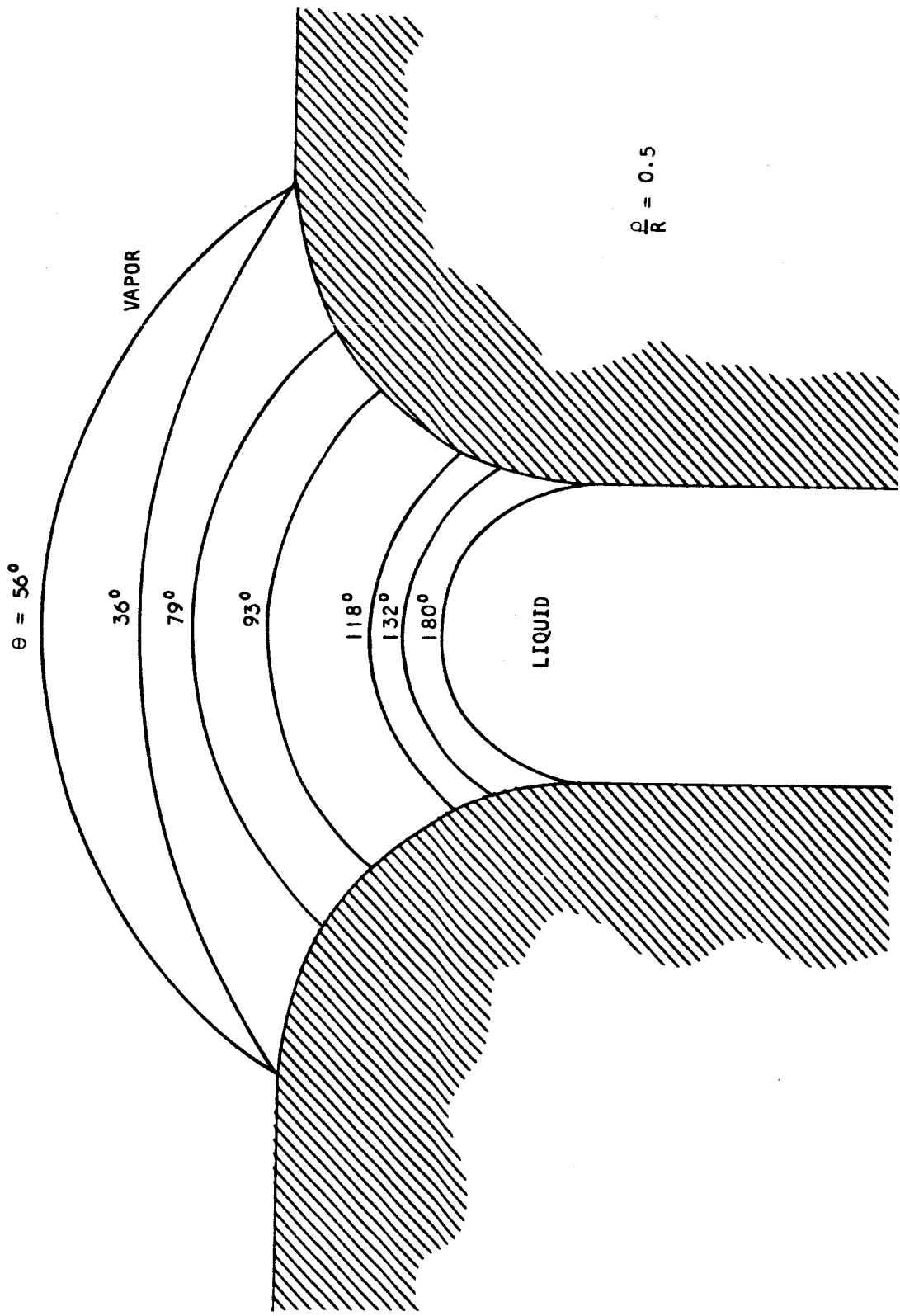$$P_B = \frac{2\sigma}{r_{max}} \sin \theta \tag{15}$$

where $r_{max} = \rho + R$

Figure 3. Normalized Breakthrough Pressure as a Function of Contact Angle and Exit Sharpness

A-21707

Figure 4. Position of Vapor Liquid Interface at Breakthrough for Various Contact Angles

$\frac{\rho}{R} = 0.5$

A-21711

Normalization yields:

$$\frac{P_B}{2\frac{\sigma}{\rho}} = \frac{\sin\theta}{\frac{\rho + R}{\rho}} = \frac{\sin\theta}{1 + \frac{R}{\rho}} \tag{16}$$

This is the equation given above defining $\frac{P_B}{2\frac{\sigma}{\rho}}$ for θ to the right of the broken line in Figure 3, and it is now seen that this occurs because for all $\theta < \theta_{max}$ in the case of liquid breakthrough ($\theta > \theta_{max}$ for vapor breakthrough) the breakoff point occurs at the pore exit extremity.

Analysis indicates that the breakthrough pressure will always be reached when the interface is at the pore exit. It is obviously impossible to support a liquid head at a rounded pore entrance for a contact angle of less than 90 deg because the surface tension always tends to pull the liquid through the pore; however, for an obtuse contact angle, the liquid vapor interface can exit at the pore entrance for pressures sufficiently less than the break-through pressure. Since it seems desirable in sublimators to have the evaporating interface near the pore exit to decrease the vapor flow length and thus the vapor pressure drop, we are interested in the pressure required to force the liquid into the pore, the break-in pressure P_{BI}.

A sketch of the pore entrance and liquid-vapor interface is shown below.
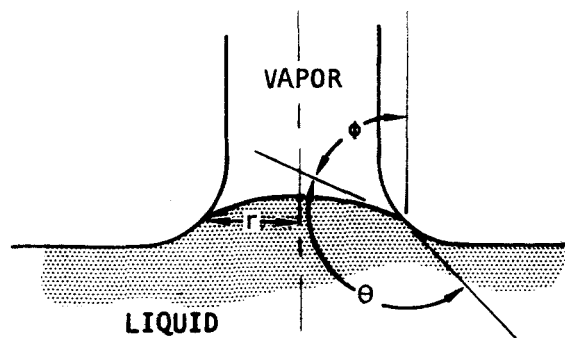
A-21706

Again, a force balance gives

$$P_L - P_V = \frac{2\sigma}{r} \cos \phi \qquad (17)$$

Since the breakin pressure is desired, the maximum value of $P_L - P_V$ must be found, and one observes that as the interface moves into the pore, r and ϕ become smaller and $\cos \phi$ becomes larger. It follows then that $P_L - P_V$ is a maximum when r is a minimum and $\cos \phi$ a maximum. This occurs when $r = \rho$, and at that point, $\phi = 180^0 - \theta$ so the normalized breakin pressure becomes:

$$\frac{P_{BI}}{2\sigma/\rho} = -\cos \theta \qquad (18)$$

This is of course true only for $\theta \geq 90^0$ since for $\theta < 90^0$ the surface tension forces pull the liquid into the pore. The normalized breakin pressure is shown as the $\rho/R = 0$ curve in Figure 3, and it is seen that this breakin pressure is always less than the breakthrough pressure, indicating that at breakthrough the interface always exists at the pore exit. Capillary tubes that will be used to experimentally verify the above analysis have been ordered.

It is seen from Figure 3 that it is indeed possible for a system to have a liquid breakthrough pressure in excess of the vapor breakthrough pressure, however this is possible only if the contact angle is greater than 90^0. It is seen also that, in general, a system which possesses a relatively high liquid breakthrough pressure will have a relatively low vapor breakthrough pressure. The one exception to this is the system with a contact angle around 90^0 for which both breakthrough pressures are nearly the same. In the sublimator application, a high liquid breakthrough pressure is desirable in order to prevent loss of water while the vapor breakthrough pressure is of little consequence. For this reason, a high contact angle seems desirable in this application. It is not necessarily true however that "the greater the contact angle the better" for as θ increases, the breakin pressure becomes closer to the breakthrough pressure, providing a narrowing band of operating pressure differential.

The question of wick dripping has not been fully answered as yet, however, it is thought that part of the explanation has to do with the bridging of liquid drops in adjacent pores. Information pertinent to the problem may be gained from capillary tube bundle tests to be performed.
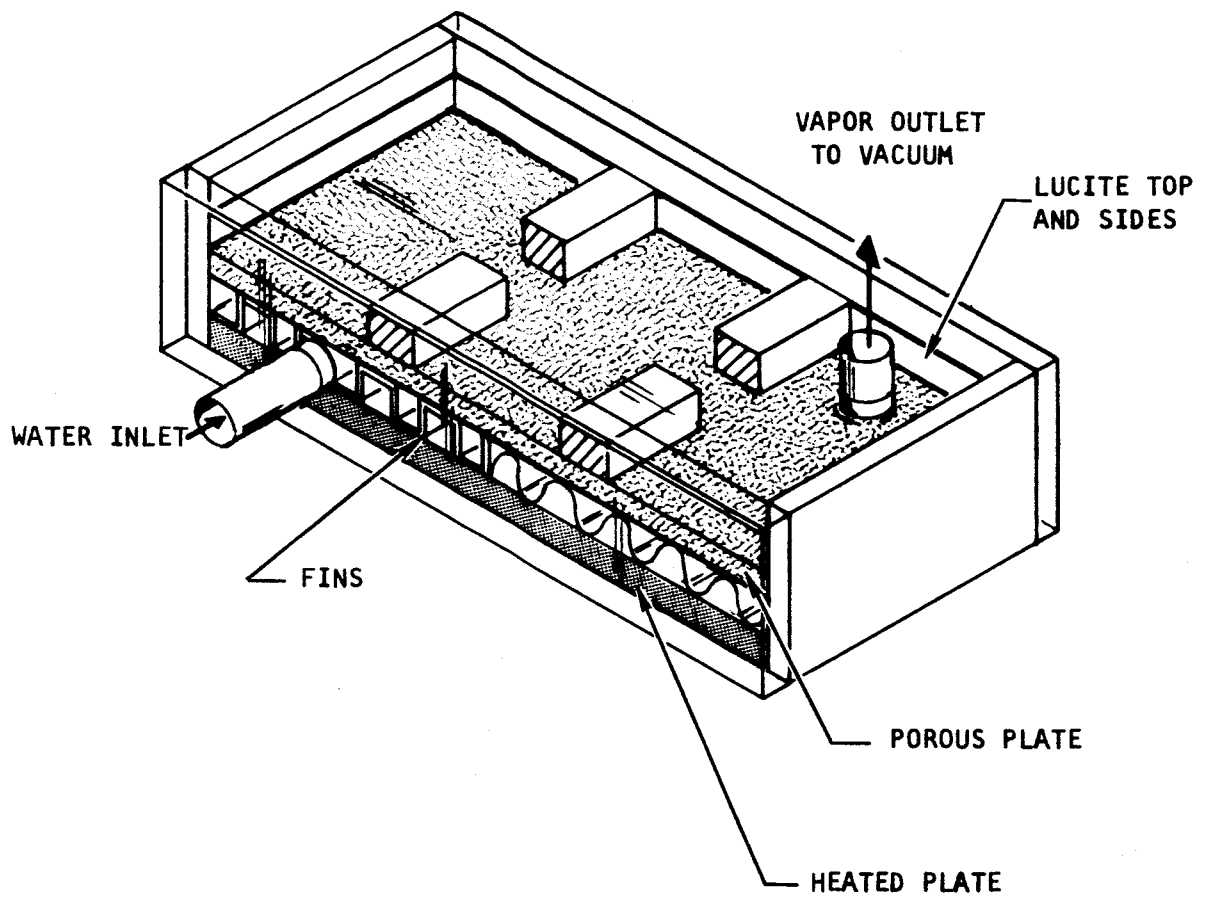
Sublimator Visualization Test

In order to obtain an optimum sublimator design, it is important to understand the mechanism of sublimator operation, and for this reason a visualization test module has been designed. It was thought that some insight might be gained into such problems as where the ice forms, whether in or out of the pores, if there is blockage of flow by fins, and what causes breakthrough and under what circumstances does it occur. With this goal in mind, the original unit, shown in Figure 5, consisting of a heated plate, finned water passage, porous plate, steam passage, and transparent sides and top was fabricated and testing was initiated.

Some difficulty was encountered in observation of the bottom porous plate surface due to the fins and the relatively small height of the water passage (0.175 in.). To alleviate this problem, a similar unit was assembled with no fins and a water passage 1/2 in. high. Figure 6 shows the new module in operation. With this unit, observation of the entire plate surface was possible and testing was continued. Photographs and movies have been taken for documentation purposes and to allow repeated observation of certain phenomena.

A schematic and photograph of the test setup are shown in Figures 7 and 8. As indicated, the water is filtered and metered before entering the water plenum. A measurable heat load is provided by passing a heated fluid through a finned passage and recording inlet and outlet temperatures. Pressures are measured at the point of water supply, in the water plenum, and in the vapor plenum. A bypass of the filter is provided in order that the flow may be reversed without destroying the filter.

Several interesting and noteworthly phenomena have been observed. When the unit is run with no heat load, a layer of ice forms over the entire bottom of the plate except along the edges of the unit. The reason for the lack of ice next to the lucite sides is probably due to heat leaking through from the surroundings. This situation is now being eliminated by the construction of another unit with thicker side plates to reduce heat conduction.

VAPOR OUTLET
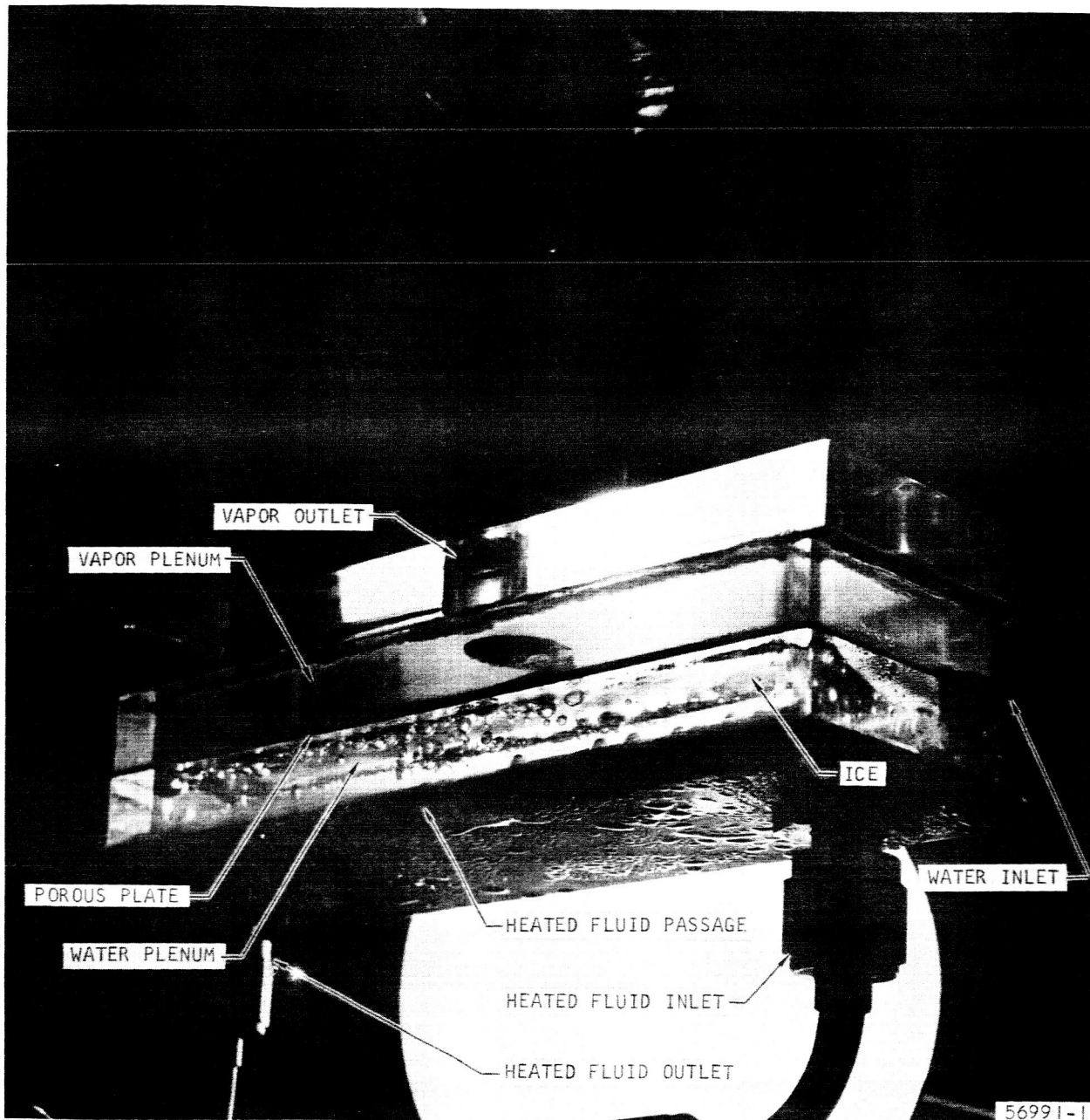TO VACUUM

LUCITE TOP
AND SIDES

WATER INLET

FINS

POROUS PLATE

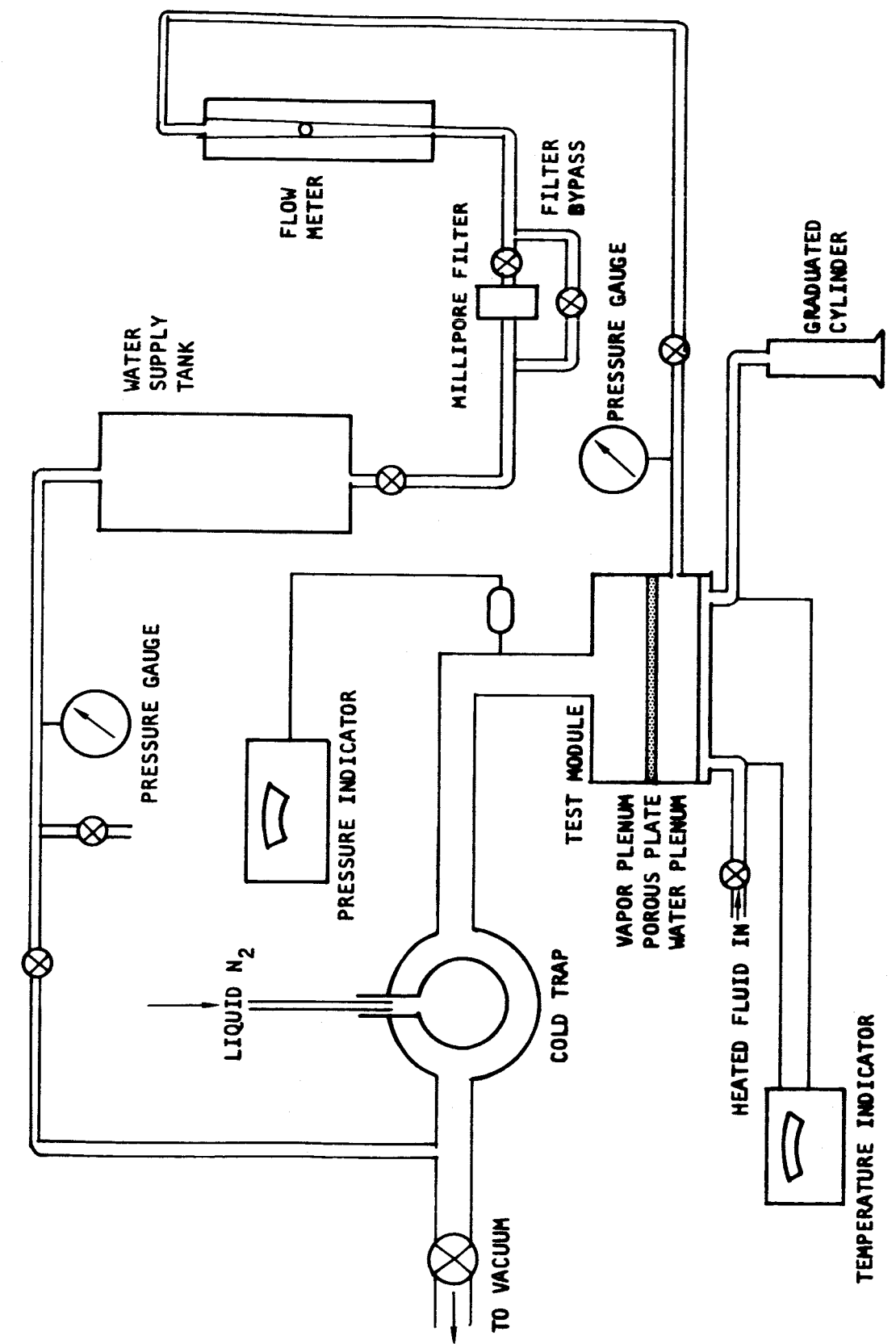HEATED PLATE

A-19936

Figure 5. Sublimation Visualization Test Unit

Figure 6.   Sublimation Visualization Test Module

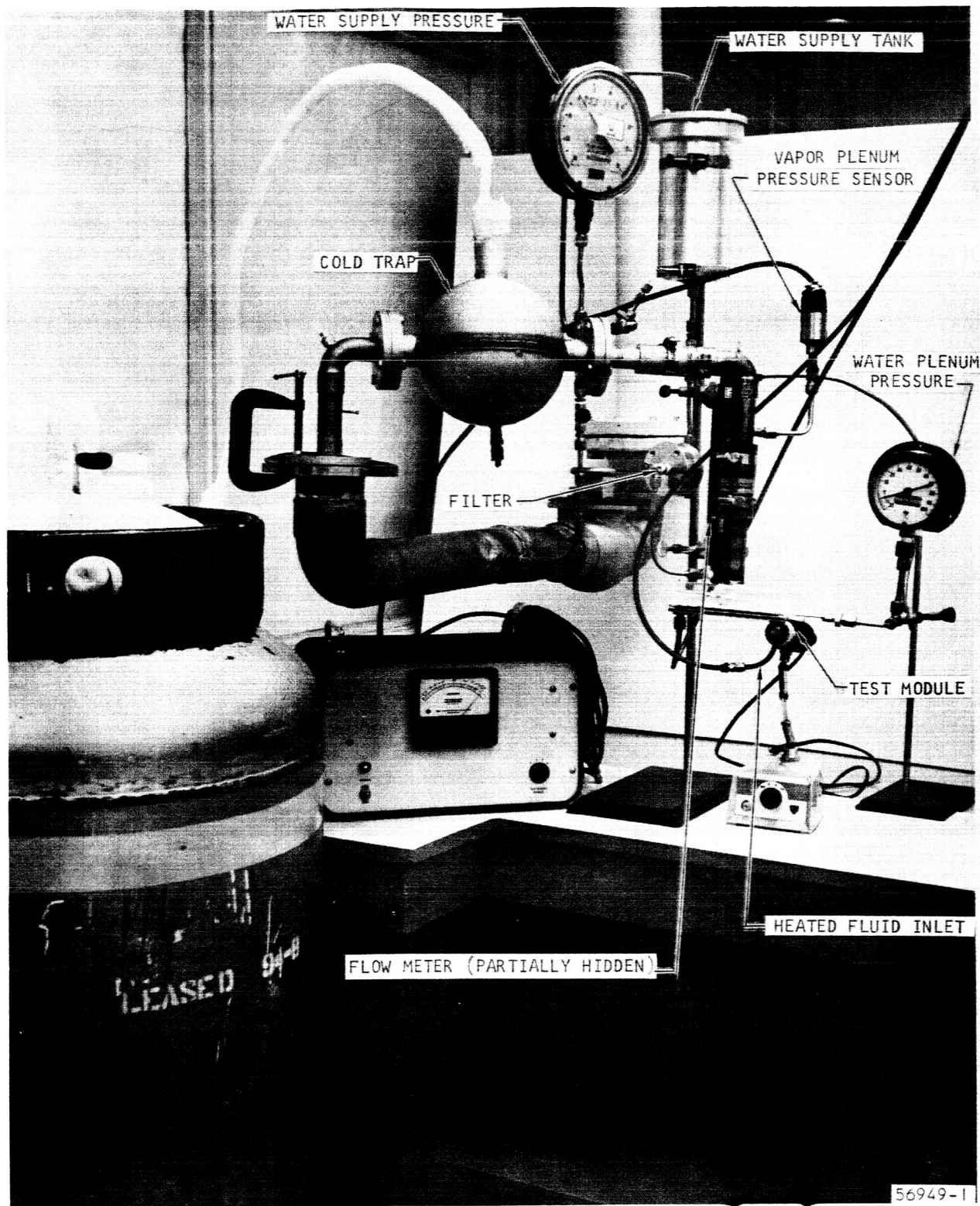Figure 7. Schematic of Sublimation Test System

A-21708
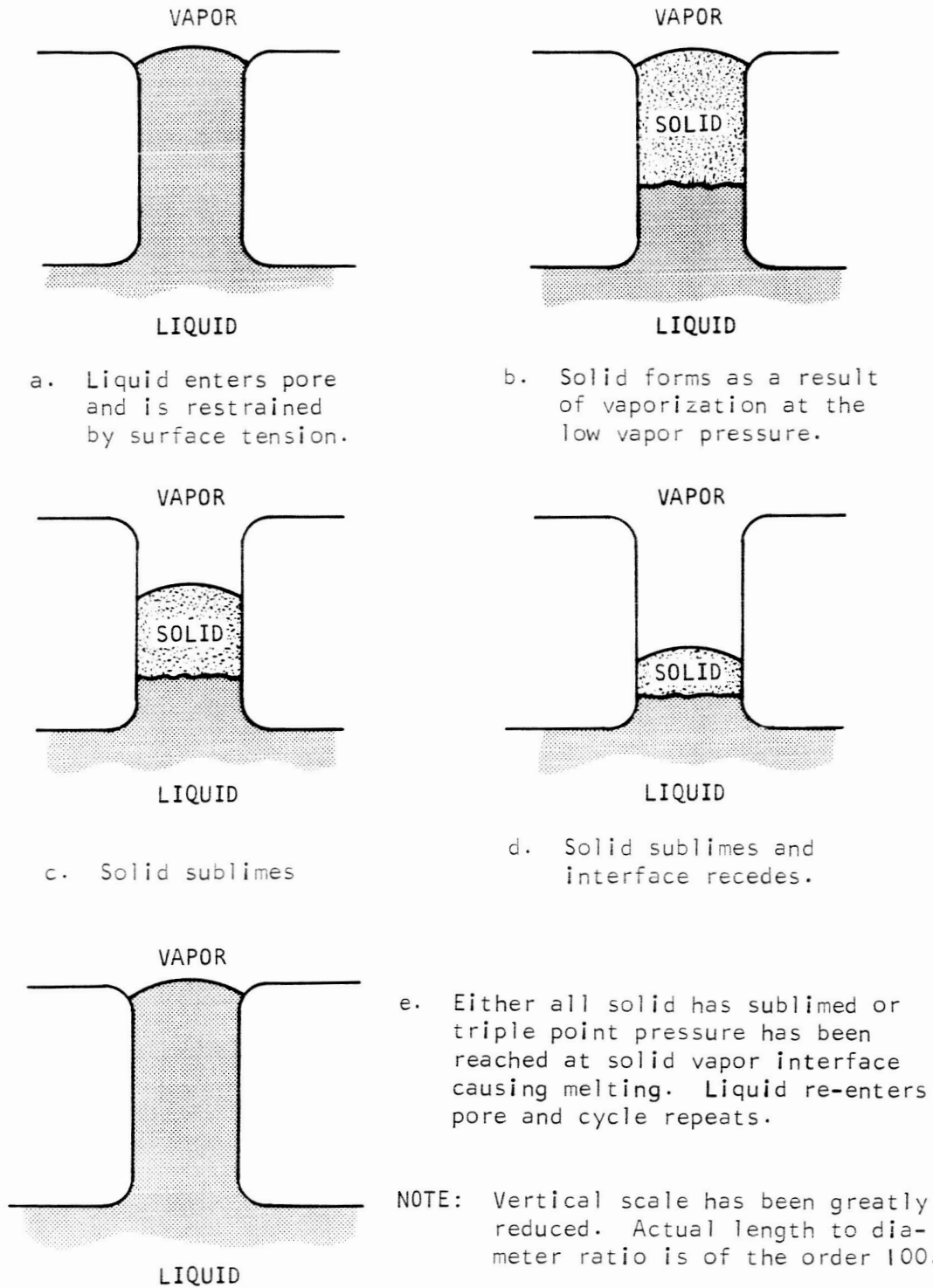
Figure 8. Sublimation Test System

Observation of the ice layer on the water passage side reveals a light colored surface, frosty in appearance, at the ice-porous plate interface. Intermittently, various light areas become darkened and when this occurs, small "fingers" of ice appear at corresponding areas on top of the plate. This change in color always proceeds from the edge of the ice layer or from an already darkened area. It is thought that the light areas are small spaces between the ice and the porous plate, formed when the ice sublimes and passes through the plate as vapor. When this space becomes sufficiently large, water rushes in, causing the darkened appearance, and some of the water passes completely through the plate, forming the "ice fingers" at the surface. This ice "break-through" occurs over only those portions of the plate which are covered with ice on the water side.

When the plate area covered by ice is reduced by increasing the heat load to the system, this intermittent breakthrough phenomenon continues over that area of the plate covered with ice but ceases to occur over areas covered with liquid water and no visible ice. Increased heat load results in the elmination of all visible ice and along with it, elimination of the formation of the "ice fingers" on the low-pressure side. If at this point the pressure on the down-stream side of the porous plate is increased while maintaining constant all other system variables, water breakthrough will occur when the pressure comes up to the triple point pressure.

This significant fact indicates that there is ice in the pores which melts when the pressure goes above the triple point, allowing water to break through. The indication of ice existing in the pores when there is no ice visible on the bottom of the plate is an important one, for an understanding of where the ice-vapor interface exists and where phase change takes place is necessary to be able to predict the vapor pressure drop which is one of the most important design considerations. Moreover the existence of ice in the pores implies a cycling mechanism in which the ice-vapor interface recedes and reforms due either to the ice melting or the interface receding all the way out of the pore and water rushing in. A series of sketches showing the possible mechanism is presented in Figure 9. In Figure a, liquid has entered the pore and is restrained at the exit by the surface tension force. Figure b shows solid which has formed in the pore as the liquid was exposed to a pressure below the triple

a. Liquid enters pore
   and is restrained
   by surface tension.

b. Solid forms as a result
   of vaporization at the
   low vapor pressure.

c. Solid sublimes

d. Solid sublimes and
   interface recedes.

e. Either all solid has sublimed or
   triple point pressure has been
   reached at solid vapor interface
   causing melting. Liquid re-enters
   pore and cycle repeats.

NOTE: Vertical scale has been greatly
      reduced. Actual length to dia-
      meter ratio is of the order 100.

A-21712

Figure 9. Possible Sublimation Mechanism When Solid Phase
           is not Visible on Liquid Side of Plate

GARRETT AIRESEARCH MANUFACTURING DIVISION

point pressure. In Figures c and d the solid phase has sublimed, causing the solid-vapor interface to recede further into the plate and also raising the absolute pressure at the interface. At this point it is thought that one of two things happens. Either the solid-vapor interface recedes until all the solid phase has sublimed or the interface pressure increases above the triple point and the solid melts, either of which would allow liquid to reenter the pore (Figure e) causing the cycle to repeat. This aspect of the sublimation process is not fully understood at this time. However, additional tests and analyses should improve this understanding.

Sublimator Performance Test Setup

Design of a fixture to be used for sublimation performance testing of various single porous plate modules was previously completed on a company-sponsored research program. The fixture design has been reviewed for improvements to yield greater flexibility and improved data and revised drawings have been made.

Test Specimen Procurement

Four sample porous plates, 3.0 in. in diameter by 0.05 in. thick, were received from Lockheed Missiles and Space Company. These plates are pure nickel and have been fabricated to yield varying porosities. It is planned to run sample evaluation tests to establish a specification for full size sublimator plates of this material. Six porous plates of various characteristics were received from the Clevite Aerospace Division. The plates are pure nickel and are rectangular, 5 in. by 7 in., 0.050 in. thick. Three pieces contain a 20 by 20 mesh 0.007 in. diameter nickel wire reinforcement screen. Use of the reinforcement screen in the parts should inhibit shrinkage during any subsequent brazing operation. One 11-in. square nickel porous plate sample was received from Union Carbide. The thickness is only 0.0072 in. which is considered to be too thin for present construction techniques. Union Carbide claims that they can fabricate the plates in thicknesses up to 0.030 in.

Porous Plate Bench Test

A complete set of detailed test instructions for porous plate bench tests was prepared. These tests are described in the AiResearch Engineering Work Order which is shown at the end of this report. Several of these tests have been performed on the Lockheed and Clevite sample plates and evaluation of the results is currently underway.

FUTURE ACTIVITIES

During the next quarter it is planned to continue on with the previously presented development plan. No changes are contemplated. Specific areas to be covered for each phase of the program are outlined below:

Water Boiler Heat Sink Module

1. Basic capillary and wicking analyses will be continued.

2. Controls analyses including water feed control and distribution will be started.

3. Single module testing designed to establish optium wick characteristics will be about 50 per cent completed.

Sublimator Heat Sink Module

1. Basic flow and capillary analysis and testing will be continued. The primary goal of this portion of the program is to obtain a better understanding of the actual sublimation mechanism.

2. Testing of single porous plates using an electrical heat source will be about 30 per cent completed. This series of tests is designed to relate sublimation performance to previously established bench test characteristics such as initial bubble point and nitrogen permeability.

Thermal Panel Development

1. Conceptual design studies are planned for the next quarter.

ENGINEERING WORK ORDER

IF REVISION: Letter ☐ **Date** _____   **Work Order No.** 3404-250017-01-0201

REQUESTED BY J. J. Killackey PROJ. 93-5	WORK ASSIGNED TO:	HOURS	MAT'L.
DATE PREPARED 4-26-66	94-5	200	300
REQUIRED COMPLETION DATE 9-30-66			
DATE CLOSED BY			

DESCRIPTION

PRODUCT NAME Porous Plate	CUSTOMER NASA Huntsville
OUTLINE NO. Study Program	SALES ORDER NO. 250017
PACKAGE OR SYSTEM NO. NASA Heat Sink Study	GOV'T. CONTRACT NO. NAS 8-11291

Detail of Work Required: **Project Identification Number** _____

RESEARCH

No Quality Control Surveillance Required

PURPOSE: Testing to be performed per this EWO is part of an over-all program to
develop an optimum porous plate sublimator heat sink heat exchanger.
A number of different types of porous plates are to be subjected to a
series of bench tests to establish plate performance characteristics.
Results of these bench tests will be correlated with the performance
data to be obtained during subsequent testing. This testing is con-
sidered to be exploratory in nature and revisions to the test procedure
outlined below will be issued when required.

PROCEDURE: Bench tests are specified below. Engineering will specify the particular
tests to be performed for each porous plate sample.

1. Initial Bubble Point in Alcohol

Prior to performing this test the plate shall be completely dry.
Thoroughly wet the porous plate by soaking it in alcohol for at least
15 minutes. Install the plate in an appropriate fixture and cover the
top surface of the plate with a layer of alcohol. The depth of the
alcohol layer shall not exceed 1/4 in. Slowly pressurize the bottom
surface of the plate with nitrogen until the first dynamic bubble
passes through the filter and rises through the liquid. The appearance
of the first true dynamic bubble is readily recognized since it is
followed by a succession of additional bubbles. Record the pressure
(in. Hg) at which the first bubble is observed. If the test is to be
repeated, thoroughly re-wet the plate by soaking in alcohol before
proceeding with the retest.

COPIES TO: I. G. Austin
T. E. McAffee
J. J. Killackey (3)
R. A. Stone
P.   Read (5)
93-5/File

---

sig   **APPROVALS**   Page 4 of 4

PROJECT ENGINEER   **OTHER**

----

2. Initial Bubble Point in Water

This test shall be performed as specified for alcohol initial bubble point
(item 1) except the plate shall be wetted by the following procedure:

a. Immerse the porous plate in a tank of distilled water.

b. Place the tank in a vacuum chamber and reduce the pressure to about
    10 mm of Hg (do not go below 5 mm of Hg). Leave the porous plate
    soak under vacuum for at least 1/2 hour.

c. The porous plate shall be removed from the water filled tank just
    prior to performing the bubble point test. The tank may be removed
    from the vacuum chamber after 1/2 hour, but the plates must be kept
    immersed until they are ready to be tested.

d. If the test is to be repeated, re-wet the plate by soaking under
    vacuum as specified above.

3. Pore Size Distribution

This test is to be performed immediately following the initial bubble
point test (alcohol and/or water) while the plate is still thoroughly
wetted. The porous plate is to be kept in the test fixture and covered
with a layer of liquid. Increase the nitrogen gas pressure until 80
per cent of the plate surface area is actively bubbling (best visual
estimate). Record the pressure (in. of Hg).

4. Surface Wetability Check

The porous plate shall be completely dry prior to performing this test.
Mount the porous plate in a horizontal position. At 4 approximately
equally spaced locations place a drop of distilled water on the plate
surface. If the plate surface is clean the drops will immediately wick
into the plate. If the plate is contaminated the water droplets will
either slowly soak into the plate or remain on top of the plate. Record
observations and note the approximately time for the water to be absorbed.
If specified, repeat the above test using alcohol, but select 4 locations
that are spaced away from the areas that have been wet with water.

5. Water Retension Pressure

The porous plate shall be completely dry prior to performing this test.
Mount the porous plate in an appropriate fixture and in a horizontal
position. Slowly fill the plenum area on the bottom surface of the porous
plate with water taking care to eliminate any trapped air pockets. After
the plenum has been filled slowly pressurize the water supply until the
first liquid droplet appears on the top surface of the porous plate; record
the liquid breakthrough pressure. Continue to increase the water pressure
until 80 per cent of the plate surface area is covered with water droplets
(best visual estimate). Record the 80 per cent pressure.

6. Water Permeability

Install the porous plate in an appropriate fixture and mount the assembly
in a horizontal position. Flow distilled and filtered water throug the
plate as noted below. Care should be taken to obtain a pressure reading
in which all liquid head effects are accounted for. Before recording the
flow verify that the inlet face of the porous plate is fully exposed to
the flow and that there are no trapped air pockets in the inlet manifold.
Test flows shall be as follows:

Water Flow, cc per min per in^2 1, 3, 5, 10, and 15 ±5 per cent
Inlet Water Temperature, ^0F Lab Ambient
Discharge Pressure   Lab Ambient

Record the water pressure drop at each flow. The plate flow area shall be
based on the active area not blocked by the test fixture. Caution: Do
not exceed a pressure differential of 20 in. of Hg across the porous
plate unless directed by Engineering.

7. Nitrogen Permeability with Discharge to Ambient

The porous plate shall be completely dry prior to performing this test.
Install the plate in an appropriate fixture and flow dry and filtered
nitrogen through the plate as specified below:

Nitrogen Flow, lb per hr ft^2 1, 2, 3, 5, and 7 ±5 per cent
Discharge Pressure   Lab Ambient
Inlet Nitrogen Temperature   Lab Ambient

Record the nitrogen pressure drop and temperature at each flow. The
plate flow area shall be based on the active flow area not blocked by
the test fixture. Caution: Do not exceed a pressure differential of
20 in. of **hg** across the porous plate unless directed by Engineering.

8. Nitrogen Permeability with Discharge to Vacuum

This test shall be as specified for nitrogen permeability with discharge
to ambient (item 7 above) except the nitrogen discharge pressure shall
not exceed 2.0 mm of Hg absolute. Record the actual discharge pressure.

NOTES:

1. Alcohol used in bubble point testing shall be Ethyl Alcohol, 95 per cent.

2. All water used in testing shall be distilled and filtered through a
   1/2 micron absolute filter prior to use.

3. All nitrogen used in testing shall be dry and free on any contaminate
   such as dirt, grit, or oil. The nitrogen shall be filtered through
   a 1/2 micron absolute filter prior to flowing through the test specimen.

4. On each plate tested record the manufacturer, lot number, serial numbe
   and all other pertinent identification information.

----

5. All testing should be performed in a clean area. When a porous plate is not actually being tested it shall be kept in a polyethylene or nylon bag at all times. This rule also applies to plates kept in a clean area.

6. Use of a vacuum oven to dry the porous plates shall be rigidly controlled. The oven shall never be used to cure epoxied assemblies or to dry a dirty or contaminated part. When porous plates are being dried other parts or assemblies may be present in the oven provided that the other parts are wet only with water or alcohol.